
Photoluminescence of $\text{Bi}_{12}\text{SiO}_{20}$ crystals

Panchenko T. V., Dyachenko A. A. and Khmelenko O. V.

Department of Physics, Electronics and Computer Science, Oles Honchar
Dnipropetrovsk National University, 72 Gagarin Avenue, 49010 Dnipropetrovsk,
Ukraine, e-mail: anna.diachenko@mail.ru

Received: 28.10.2015

Abstract. Spectra of photoluminescence (PL), luminescence excitation, stationary and photoactivated optical absorptions and photoconductivity are studied for $\text{Bi}_{12}\text{SiO}_{20}$ crystals. The PL spectra contain wide bands, of which shapes differ for the cases of electronic valence-to-conduction band excitation (the photon energies $h\nu = 3.3\text{--}4.0$ eV) and the excitation occurring from the impurity absorption band ($h\nu = 2.8\text{--}2.9$ eV). The photochromic effect and the induced impurity photoconductivity are also observed. Recombination and intra-centre mechanisms of the PL are discussed.

Keywords: photoluminescence, optical absorption, photoconductivity, recombination centres, $\text{Bi}_{12}\text{SiO}_{20}$ crystals

PACS: 42.70.+a; 78.55.+m

UDC: 535.3

1. Introduction

Photorefractive $\text{Bi}_{12}\text{SiO}_{20}$ (BSO) crystals belong to a family of sillenites with the general chemical formula $\text{Bi}_{12}\text{MO}_{20}$ (or BMO, where $M = \text{Si, Ge, Ti}$ or some other elements). Sillenites combine the properties of both active dielectrics and wide-gap semiconductors, their bandgap width being equal to $\Delta E_g \approx 3.4$ eV at the temperature $T = 4.2$ K. The BSO crystals are employed as functional materials in the devices aimed at recording, handling and storage of optical information. The processes of photogeneration of electrons, their distribution over the local levels in the bandgap, as well as formation, due to a photochromic effect (PCE), of photoinduced colour centres, take an important part in functioning of these devices.

The local levels in the bandgap are due to intrinsic point defects, or centres, available in BSO. The structure of the shallow bandgap levels with the thermal activation energy $E_a^T \leq 1.3$ eV, which are responsible for attachment and capture of charge carriers (electrons), has been studied in details with the techniques of thermal activation spectroscopy. This structure is rather complex [1, 2]. Besides, the existence of deep levels, with the energy of optical activation $E_a^O \approx 2.6\text{--}3.0$ eV, has been evidenced by spectral studies of the photoconductivity and the optical absorption in BSO. These levels are responsible for electron generation, providing a high 'extrinsic' photoconductivity and a 'shoulder' of the absorption profile near the fundamental absorption edge in BSO [3–5]. Magneto-optical and PCE studies have revealed that the intra-centre transitions taking place in the Bi–O complexes also contribute to the absorption shoulder [4, 6].

On the other hand, a number of effects (e.g., thermal activation and extinction of the photoconductivity, and non-stability of the characteristics of optical holographic recording [3, 7, 8]) have been observed in the sillenites, of which understanding requires some information about recombination centres. In this case photoluminescence (PL) studies can be useful. Nonetheless, the PL in the sillenite has still not been studied in sufficient detail. Some spectral characteristics of the

luminescence have been reported in Refs. [1, 5, 9] and, in particular, it has been shown that its intensity drops drastically when the temperature increases from 80 to 300 K [1]. At the same time, the problem of the physical nature of the recombination centres remains under discussion.

In the present work, we describe the results of PL studies for the BSO crystals, which are complemented by the analyses of the optical absorption spectra and the photoconductivity.

2. Experimental

The BSO crystals were grown with the Czochralski method along the crystallographic direction [001]. The samples for spectroscopic studies were prepared in the shape of polished plates with the thicknesses $d = 0.12\text{--}5.0$ mm and the squares 8×8 mm² in the (001) planes. For the photoelectric measurements, Ag-electrodes were deposited onto one of (001) planes, with the gaps being 0.7–1.0 mm.

The PL was excited from a sample bulk, using a xenon radiation obtained from DKsEI-1000 lamp. It was detected perpendicular to the propagation direction of the exciting incident light. Dependences of the radiation intensity on the wavelength λ were recorded for the cases of PL spectra $I^{PL}(\lambda)$ and PL excitation (PLE) spectra $I^{PLE}(\lambda)$ in the region $\lambda = 0.3\text{--}1.0$ μm .

An automated measuring complex was used in our experiments. Selective excitation was provided by a diffraction monochromator MDR-4. For excluding red and IR irradiation, a filter based on a saturated solution of CuSO₄ in water was used. To detect radiation, we employed a diffraction monochromator MDR-12 with a step motor (the resolution 0.02 nm) and a photoelectron amplifier FEU-136 equipped with a cooling system, which was operated in the quantum counting regime. After amplification, a signal from FEU-136 came to a discriminator, and then to a counter. Control of the spectral complex and its connection with a computer was performed using a standard CAMAC system. Most of the measurements were fulfilled at the temperatures $T = 4.2 \pm 0.2$ and 80 K. The $I^{PL}(\lambda)$ and $I^{PLE}(\lambda)$ dependences were represented as functions of the light photon energy $h\nu$, $I^{PL}(h\nu)$ and $I^{PLE}(h\nu)$ (with $\nu = 1/\lambda$), after taking into account the conservation conditions for the radiation flux: $dN_1 = I^{PL}(\lambda)d\lambda = -I^{PL}(h\nu)d h\nu$ and $dN_2 = I^{PLE}(\lambda)d\lambda = -I^{PLE}(h\nu)d h\nu$.

The spectra of stationary ($t_0(h\nu)$) and photoinduced ($t^{ph}(h\nu)$) optical transmissions were measured using a spectrophotometer Cary-4E. The photoinduced state was excited by a dark-blue light. Besides, we measured the spectra of stationary ($\alpha_0(h\nu)$) and photoinduced ($\alpha^{ph}(h\nu)$) absorptions, as well as the spectra $\Delta\alpha^{ph}(h\nu) = \alpha^{ph}(h\nu) - \alpha_0(h\nu)$ that characterize the optical absorption variations due to PCE excitation. The absorption spectra were calculated with the technique described in Ref. [10].

The photoconductivity was measured using a monochromator SPM-2 (the resolution ~ 0.02 eV), a standard technique for synchronous detection, and a voltmeter-electrometer B7-30. The measurements were carried out under a constant electric field and the light was modulated with the frequency of 12 Hz. We collected the following spectra: (i) the stationary conductivity $\Delta\sigma^{ph}(h\nu) = \sigma_0^{ph}(h\nu) - \sigma^T(h\nu)$, (ii) the photoconductivity after activation of samples by the dark-blue light, $\Delta\sigma^{phi}(h\nu) = \sigma^{phi}(h\nu) - \sigma^T(h\nu)$, and (iii) the induced photoconductivity, $\Delta\sigma^{IPC}(h\nu) = \sigma^{phi}(h\nu) - \sigma_0^{ph}(h\nu)$, where $\sigma_0^{ph}(h\nu)$, $\sigma^{phi}(h\nu)$ and $\sigma^T(h\nu)$ imply the electric conductivities under the conditions of irradiation, dark-blue activation and darkness, respectively. All the spectra were normalized with respect to the instrument function of photon flux spectral distribution.

The optical absorption and the photoconductivity were studied in the photon energy region $h\nu = 0.5\text{--}3.4$ eV at $T = 80$ and 290 K. A xenon lamp DKSSh-600 W with a light filter ($h\nu^{act} \approx 2.8\text{--}2.9$ eV) were used for photoactivating. Individual components of the spectral contours were separated using a technique borrowed from Ref. [11].

3. Results and discussion

PL in the BSO crystals is observed in the region $h\nu = 1.0\text{--}2.9$ eV. The spectral shape $I^{PL}(h\nu)$ depends notably on the exciting photon energy $h\nu^{exc}$ (see Fig. 1a, curves 4 to 8), though it does not change while the temperature increases from 4.2 up to 80 K.

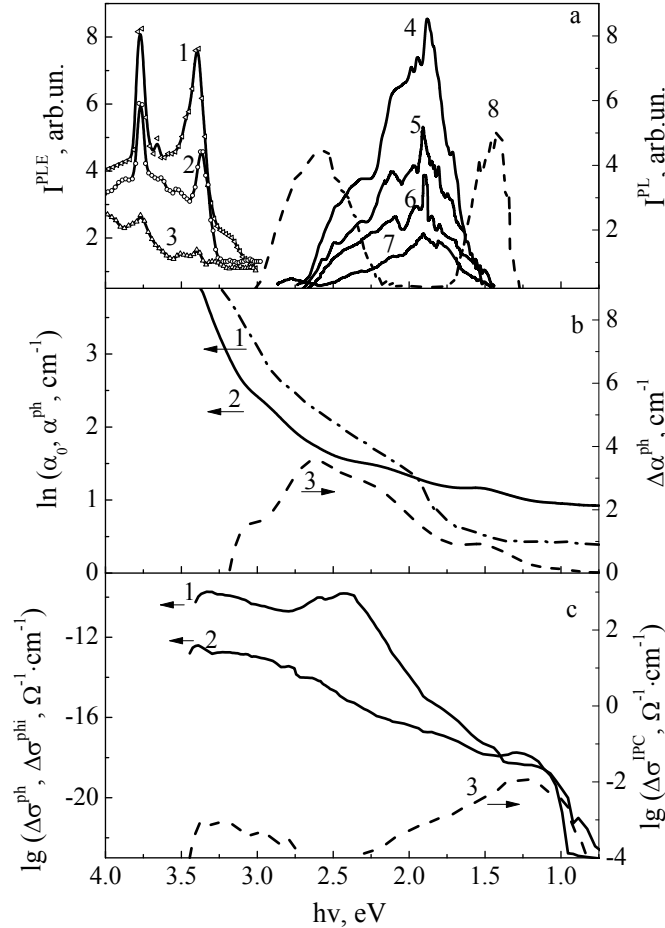


Fig. 1. (a) Spectra of PL excitation $I^{PLE}(h\nu)$ in the bands with $h\nu_{max} = 1.9$ (curve 1), 2.1 (curve 2) and 2.35 (curve 3) eV, and PL spectra $I^{PL}(\lambda)$ under light excitation with $h\nu^{exc} = 3.35$ (curve 4), 3.7 (curve 5), 3.6 (curve 6), 3.52 (curve 7) and 2.8 (curve 8) eV ($T = 4.2$ K). (b) Spectra of stationary ($\alpha_0(h\nu)$, curve 1) and photoinduced ($\alpha^{ph}(h\nu)$, curve 2) absorptions and PCE spectrum ($\Delta\alpha^{ph}(h\nu)$, curve 3), as measured at $T = 290$ (curve 1) and 80 K (curves 2 and 3). (c) Spectra of stationary conductivity ($\Delta\sigma^{ph}(h\nu)$, curve 2), photoconductivity ($\Delta\sigma^{phi}(h\nu)$, curve 1) and induced photoconductivity ($\Delta\sigma^{IPC}(h\nu)$, curve 3) measured after UV activation at $T = 290$ (curve 2) and 80 K (curves 1 and 3).

Under excitation with $h\nu^{exc} \geq 3.4$ eV, i.e. below the fundamental absorption edge energy for the BSO, the $I^{PL}(h\nu)$ spectra occupy the region $\Delta h\nu_1 = 1.5\text{--}2.7$ eV. This is a so-called ‘PL of the type I’. The spectra involve broad structured bands consisting of five components, with the halfwidths $\Delta h\nu \approx 0.010\text{--}0.024$ eV and the positions $h\nu_{max,1}$ of maxima equal to 1.72, 1.90, 2.10, 2.36 and 2.52 eV. The long-wavelength tail of the $I^{PL}(h\nu)$ curve is characterized by narrow equidistant maxima. The corresponding distances are $\Delta_1 h\nu = 0.063$ eV, which coincides with the excitation energy of the longitudinal optical phonons for the BSO crystals (508 cm^{-1} – see ref. [12]). The intensities of the components decrease with decreasing $h\nu^{exc}$. The most intense component with $h\nu_{max} = 1.9$ eV has also been observed in Ref. [9]. However, the whole set of the

spectral PL components is shifted towards the short-wavelength region, when compared to the components with $h\nu_{\max} = 1.77, 1.46, 1.3$ and 1.17 eV obtained in Ref. [1]. In contrast to the results obtained in Ref. [1], the main contribution to our $I^{PL}(h\nu)$ spectra stems from the low-energy components rather than from the high-energy ones.

The selective excitation spectra $I^{PLE}(h\nu)$ for the spectral PL components of the type I are identical and look like doublets consisting of narrow bands with $h\nu_{\max} = 3.75$ and 3.4 eV. A weakly pronounced band with $h\nu_{\max} = 3.65$ eV appears in the tail of the first narrow band (see Fig. 1a, curves 1 to 3). The Stokes shift between the spectral bands $I^{PLE}(h\nu)$ and the components of the $I^{PL}(h\nu)$ spectra amounts to 1.25 – 2.0 eV. Such a significant shift has earlier been marked as a feature characteristic for the PL in many Bi-containing compounds [1, 13, 14]. A narrow peak located at $h\nu_{\max} = 3.39$ eV, in which practically all the PL is excited, has also been observed in Refs. [1, 5]. On the other hand, no information has ever been reported concerning the availability of peaks with $h\nu_{\max} = 3.75$ and 3.65 eV.

Under the excitation with $h\nu^{exc} \approx 2.8$ – 2.9 eV (i.e., in the tail of the fundamental optical absorption band for BSO – see Fig. 1b, curves 1 and 2) we have found the two PL bands located in the regions $h\nu_2 = 2.0$ – 2.9 eV and $h\nu_3 = 1.0$ – 1.7 eV. We term the latter as a ‘PL of the type II’. The first band includes the components peaked at the energies $h\nu_{\max,2}$ equal to $2.76, 2.55$ and 2.34 eV and the halfwidths $\Delta h\nu \approx 0.01$ – 0.023 eV, whereas the second band comprises two components ($h\nu_{\max,2} = 1.52, 1.4$ eV and $\Delta h\nu \approx 0.010$ – 0.018 eV – see Fig. 1a, curve 8).

Note that changes in the shape of the PL spectra occurring under decreasing excitation energy (from $h\nu^{exc} \geq 3.4$ eV down to $h\nu^{exc} \approx 2.8$ eV) have already been observed in $\text{Bi}_{12}\text{GeO}_{20}$ crystals [5]. The different shapes of the $I^{PL}(h\nu)$ spectra are caused by specific excitation conditions, thus indicating different physical mechanisms for the PL of the types I and II.

For further discussion of our results it is necessary to take into consideration the peculiarities of energy band structure in the BSO crystals, as well as the specific features of their optical absorption and photoconductivity. It has been shown in Refs. [15, 16] that both the conduction and valence bands are mainly due to the structural complexes of bismuth oxide. Namely, the conduction band is formed by the $6p$ -orbitals of bismuth and the valence band by the p -orbitals of oxygen. The latter band consists of three subbands, electron transitions from which into the conduction band result in a characteristic triplet ($3.55, 3.65$ and 3.75 eV) in the near-UV range. The corresponding peaks have been observed in the reflection spectra [16]. The triplet mentioned above is also present in our $I^{PLE}(h\nu)$ spectra: the peak centred at 3.75 eV is the most intense, that located at 3.65 eV peak is weakly expressed, while the peak 3.55 eV is somewhat shifted ($h\nu_{\max} = 3.4$ eV). Its spectral position corresponds to a sharp increase in the stationary optical absorption and to the peak of intrinsic photoconductivity observed at 80 K (see Fig. 1), i.e. it determines the low-temperature width of the bandgap in BSO. A shift of the peak usually observed at $h\nu_{\max} = 3.55$ eV may be caused by the indirect-band mechanism of the optical transitions [17].

Since the PL of the type I is excited owing to the electron transitions from the valence subbands into the conduction band, it would be natural to assume a recombination mechanism for this PL. This mechanism is also supported by a significant width of the spectral curve $I^{PL}(h\nu)$, whereas for the $I^{PLE}(h\nu)$ spectra this is evidenced by a presence of the band localized near the fundamental absorption edge and a correlation of its location with that of the peak of the intrinsic photoconductivity. The measurements of the PL spectra excited in the band located at $h\nu = 3.4$ eV under different PL-detection delays $\Delta\tau$ relative to the exciting light pulse have shown that the PL intensity drops drastically (by about two orders of magnitude) already at $\Delta\tau > 10^{-3}$ s. This fact does not contradict the recombination mechanism, too (see Ref. [1]). In this case, the electron states of the recombination centres are strongly influenced by the crystalline lattice, and the spectral

positions of the PL bands depend on crystalline material and its bandgap. Indeed, in the PLE spectra of $\text{Bi}_4\text{Ge}_3\text{O}_{12}$ crystals with a wide enough bandgap ($\Delta E_g = 4.35$ eV) the PL spectrum shifts towards the UV range ($\Delta h\nu = 3.10\text{--}1.77$ eV), with a maximum occurring near 2.48 eV. Moreover, a clear link between the short-wavelength PL bands and the local levels in the bandgap has been established [13]. Important additional evidences to the recombination mechanism of the PL of the type I in BSO can be obtained from the studies of its kinetics, which are now in progress.

One has to take into consideration intense temperature quenching of the PL of the type I [1] and temperature activation of the intrinsic photoconductivity with increasing temperature up to 300 K [3], on the one hand, and increase in the intensity of this PL and temperature quenching of the photoconductivity of BSO at $T \leq 80$ K (see Fig. 1c, curves 1 and 2), on the other hand. Temperature activation and quenching of both the photoconductivity and the PL can be described in the framework of a multi-centre recombination model for broad-band n -type semiconductors [18], where the photoconductivity is controlled by s -centres of rapid recombination and r -centres of slow recombination. These centres differ in the cross-sections of electron capture ($C_r/C_s \ll 10^{-3}$) and in their energy positions inside the bandgap (the r -centres are closer to the top of the valence band than the s -centres.) Adhesion of non-equilibrium charge carriers, electrons in our case, to the t -levels near the bottom of the conduction band should also be taken into account. With increasing temperature, the t -levels become empty and the electrons from the conduction band get onto the s -centres, thus blocking the channels of rapid regeneration. As a consequence, the photoconductivity increases, the PL through the s -centres is quenched, while the PL component channelled through the r -centres is enhanced. Probably, this is the reason why the PL of the type I is quenched and the IR-luminescence occurs in the BSO crystals at $T = 300$ K, as observed in Ref. [1]. On the contrary, at low temperatures the free s -centres provide a clear experimental observation of the PL of the type I and a decrease in the intrinsic conductivity (see Fig. 1a, c). In this case the spectral positions of the PL components of the type I define the optical activation energy for the s -centres. In this manner we obtain E_a^O equal to 1.75, 1.9, 2.1, 2.36 and 2.52 eV.

The large Stokes shift of both the PL and the PLE components, $\Delta E_{St} \approx 1.25\text{--}2.0$ eV, as well as their significant halfwidths, point to strong electron-phonon interactions. The latter may be estimated by the Huang-Rhys factor, $S_{HR} = \Delta E_{St}/2h\nu^{ph} = 10\text{--}17$, which in our case is substantially larger than the same parameter typical for many semiconductors (e.g., one has $S_{HR} = 2.66$ eV for GaAs and $S_{HR} = 1.44$ eV for InSb [19]). The large Stokes shift may take place in the crystals with significant ionic degrees of bonds. A relevant theoretic analysis [20] has demonstrated that, in the case of BMO, this is caused by a strong hybridization of Bi $6p\text{--}O(1)2p$ -states in the Bi-(O1) sublattice.

The PL of the type II is excited by the light from the regions of the absorption shoulder and of the maximal extrinsic photosensitivity in BSO, so that we have $h\nu^{exc} = 2.8\text{--}2.9$ eV $\approx h\nu^{act}$. In other words, the photochromic effect is accompanied by the emission caused by appearance of the photoinduced colour centres (see Fig. 1a, b). It has been revealed that these centres occur as a result of changes in the charge states of the non-stoichiometric $\text{Bi}^{3+}_{\text{Si}}$ and $\text{Bi}^{5+}_{\text{Si}}$ ions substituting Si^{4+} ions in the oxygen tetrahedra of BSO via the following scheme: $\text{Bi}^{5+}_{\text{Si}} + e \rightarrow \text{Bi}^{4+}_{\text{Si}} + e \rightarrow \text{Bi}^{3+}_{\text{Si}}$ [4, 6]. The model of the intrinsic defects in BMO suggesting a trivalent and pentavalent bismuth in the Si or Ge positions has been developed in Ref. [21]. It has been successfully used while synthesizing new sillenites, in which the M-positions are occupied by various pairs of trivalent and pentavalent ions [22]. This model has also been engaged in the explanation of basic physical properties of BMO [23]. Moreover, the presence of $\text{Bi}^{3+}_{\text{Si}}$ ions has been firmly established using the neutron-diffraction structural studies for the BMO crystals [24].

The relations between the intensity increase (or decrease) for the PCE bands and the excess

(or lack) of bismuth in the BMO crystals with non-stoichiometric compositions have been ascertained in Ref. [4]. The availability of the paramagnetic centres $\text{Bi}_{\text{Si}}^{3+} + h$ (with h denoting the holes located in the nodes of GeO_4 oxygen tetrahedra) has been found in thermally decolorized $\text{Bi}_{12}\text{GeO}_{20}$ crystals after their photoactivation with the photons $h\nu = 2.8\text{--}2.9$ eV, using the methods of magnetic circular dichroism and the optical detection of magnetic resonance [6]. It is natural to assume that the $\text{Bi}_{\text{Si}}^{3+}$ ions are formed due to reducing of the $\text{Bi}_{\text{Si}}^{5+}$ ions. The PCE spectrum in the region $h\nu = 2.30\text{--}3.1$ eV contains the four individual components located at 2.37, 2.65, 2.90 and 3.08 eV (see Fig. 1b, curve 3). They correspond to the optical transitions in tetrahedral oxygen complexes $\text{Bi}_{\text{Si}}^{3+} - \text{O}^-$, which are generically related to the transitions $^1\text{S}_0 \rightarrow ^1\text{P}_1$ and $^1\text{S}_0 \rightarrow ^3\text{P}_1$ between the energy levels of the free Bi^{3+} ion. In this case, the absorption associated with the component located at $h\nu_{\text{max}} = 2.9$ eV in the PCE spectrum may be accompanied by the emission occurring in the components with $h\nu_{\text{max}} = 2.76, 2.55, 2.34$ eV in the PL spectrum.

Hence, the PL of the type II represents, most probably, an intra-centre luminescence. The absence of correlations among the band positions in the PCE and IPC spectra (see Fig. 1b, c, curve 3) is also in favour of this conclusion. The latter fact indicates that the electrons are redistributed over deep and shallow levels in the bandgap, as a result of photoactivation of BSO by the light with the photon energy $h\nu^{\text{act}} = 2.8\text{--}2.9$ eV. The nature of the second band in the PL of the type II needs further studies.

4. Conclusions

Summarizing the main results of this work, we have studied different spectral characteristics of the PL and the PL excitation for the BSO crystals. Basing on our data obtained for the PL spectra, the photochromic effect and the induced extrinsic photoconductivity, we have demonstrated the following:

- (i) The PL excited inside the region of the optical transitions ‘valence-to-conduction band’ in BSO has the recombination character; it can be described in the framework of the multi-centre recombination model;
- (ii) The PL excited in the region of the high-energy band in the PCE spectrum has the intra-centre nature, while the $\text{Bi}_{\text{Si}}^{3+} - \text{O}^-$ complexes can well represent the recombination centres.

References

1. Malinovsky V K, Gudayev O A and Gusev V A. Photoinduced phenomena in sillenites. Novosibirsk: Nauka (1990).
2. Panchenko T V and Snezhnoy G V, 1993. Electrically active defects in nondoped and doped by Al and Ga crystals $\text{Bi}_{12}\text{SiO}_{20}$. *Fiz.Tv.Tela.* **35**: 2945–2958.
3. Panchenko T V and Yanchuk Z Z, 1996. Photoelectrical properties of $\text{Bi}_{12}\text{SiO}_{20}$ crystals. *Fiz.Tv.Tela.* **38**: 2018–2028.
4. Panchenko T V, Truseeva N A and Osetsky Yu G, 1992. Color centers in $\text{Bi}_{12}\text{SiO}_{20}$ crystals. *Ferroelectrics.* **129**: 113–118.
5. Grabmaier B and Oberschmid R, 1986. Properties of pure and doped $\text{Bi}_{12}\text{GeO}_{20}$. *Phys. Stat. Solidi (a).* **96**: 199–210.
6. Briat B, Reyher H, Hamri A, Romanov N, Launay J and Ramaz F, 1995. Magnetic circular dichroism and the optical detection of magnetic resonance for the Bi antisite defect in $\text{Bi}_{12}\text{GeO}_{20}$. *J. Phys.: Condens. Matter.* **7**: 6951–6959.
7. Grachev A I, 1999. Holographic recording in photorefractive crystals with nonstationary and nonlinear photoconductivity. *Phys. Sol. State.* **41**: 922–927.

8. Plesovskikh A M, Shandarov S M and Ageev E Yu, 2001. Dynamics of photorefractive response in sillenite crystals with double ionized donor centers and shallow traps. Phys. Sol. State. **43**: 251–254.
9. Hou S L, Lauer R B and Aldrich R E, 1973. Transport processes of photoinduced carriers in $\text{Bi}_{12}\text{SiO}_{20}$. J. Appl. Phys. **44**: 2654–2658.
10. Panchenko T V, 1998. Thermo-optical investigation of deep levels in doped crystals $\text{Bi}_{12}\text{SiO}_{20}$. Phys. Sol. State. **40**: 415–419.
11. Glebovsky D N, Krashennnikov A A, Bedrina M E and Zalikman P I, 1981. On the problem of approximate separation of complex spectral contour into individual constituents. Zhurn. Prikl. Spectrosk. **35**: 513–515.
12. Golubovic A and Nikolic S, 2002. The growth and optical properties of $\text{Bi}_{12}\text{SiO}_{20}$ single crystals. J. Serb. Chem. Soc. **67**: 279–289.
13. Petrov S A, Chetvergov N A and Nuriyev E I, 1986. Some peculiarities of bismuth orthogermanate photoluminescence. Fiz.Tv.Tela. **28**: 3540–3541.
14. Pynenkov A A, Firstov Sergei V, Panov A A, Firstova E G, Nishchev K N, Bufetov Igor' A and Dianov Evgenii M, 2013. IR luminescence in bismuth-doped germanate glasses and fibres. Quantum Electronics. **43**: 174–176.
15. Efindeev Sh M, Mamedov A M and Bagiev V E, 1988. Reflection UV-spectra of $\text{Bi}_{12}\text{TiO}_{20}$ single. Fiz.Tv.Tela. **30**: 3169–3171.
16. Dovgiy Ya O, Zamorsky M K, Mikhailin V V and Kolobanov V N, 1986. Analysis of optical functions of $\text{Bi}_{12}\text{SiO}_{20}$ single crystals. Izvestiya Vysshikh Uchebnykh Zavedeniy. **4**: 110–112.
17. Panchenko T V and Kopylova S Yu, 1995. Edge absorption in $\text{Bi}_{12}\text{SiO}_{20}$ crystals. Fiz.Tv.Tela. **37**: 2578–2586.
18. Lashkaryov V I, Lubchenko A I and Sheikman M K. Nonequilibrium processes in photoconductors. Kiev: Naukova dumka (1988).
19. Ridley B. Quantum processes in semiconductors. Moscow: Mir (1986).
20. Kalinkin A I, Skorikov V M and Soldatov A A, 1992. Electronic structure of $\text{Bi}_{12}\text{GeO}_{20}$. Neorganicheskie Materialy. **28**: 558–561.
21. Craig D C and Stephenson N S, 1975. Structural study of some body-centered cubic phases of mixed oxides involving Bi_2O_3 : The structures of $\text{Bi}_{25}\text{FeO}_{40}$ and $\text{Bi}_{38}\text{ZnO}_{60}$. J. Solid State Chem. **15**: 1–8.
22. Kargin Yu F, Mar'in A A and Skorikov V M, 1982. Crystal chemistry of piezoelectric with sillenite structure. Izv.AN SSSR. Neorganicheskie Materialy. **18**: 1605–1614.
23. Oberschmid R, 1985. Absorption centers of $\text{Bi}_{12}\text{GeO}_{20}$ and $\text{Bi}_{12}\text{SiO}_{20}$ crystals. Phys. Stat. Solidi (a). **89**: 263–270.
24. Radaev S F and Simonov V I, 1992. Sillenite structure and atomic mechanism of substitution therein. Kristallografiya. **37**: 914–944.

Panchenko T. V., Dyachenko A. A. and Khmelenko O. V. 2016. Photoluminescence of $\text{Bi}_{12}\text{SiO}_{20}$ crystals. Ukr.J.Phys.Opt. **17**: 39 – 45.

***Анотація.** Досліджено спектри фотолюмінесценції (ФЛ) і збудження люмінесценції, стаціонарних і фотоактивованих оптичного поглинання і фотопровідності в кристалах $\text{Bi}_{12}\text{SiO}_{20}$. Спектри ФЛ містять широкі смуги, форма яких відрізняється для випадків електронного збудження за схемою валентна зона–зона провідності (енергія фотонів $h\nu = 3.3\text{--}4.0\text{ eV}$) і збудження зі смуги домішкового поглинання ($h\nu = 2.8\text{--}2.9\text{ eV}$). Спостережено також фотохромний ефект та індуковану домішкову фотопровідність. Обговорено рекомбінаційний і внутріцентровий механізми ФЛ.*